

# Effects of norepinephrine-induced activation of rat vascular adventitial fibroblasts on proliferation and migration of BMSCs involved in vascular remodeling

JUN GAO<sup>1\*</sup>, LI LI<sup>2\*</sup>, DONGLI ZHOU<sup>3\*</sup>, XUHONG SUN<sup>4</sup>, LILU CUI<sup>4</sup>, DONGLIN YANG<sup>4</sup>,  
XIAOHUI WANG<sup>4</sup>, PENGCHAO DU<sup>4</sup> and WENDAN YUAN<sup>4</sup>

<sup>1</sup>Medical Laboratory and <sup>2</sup>Pediatric Department, Yantai Affiliated Hospital of Binzhou Medical University, Yantai, Shandong 264100; <sup>3</sup>Nurse's Office, Health School of Laiyang, Laiyang, Yantai, Shandong 265200; <sup>4</sup>Institute of Pathology and Pathophysiology, Basic Medical School, Binzhou Medical University, Yantai, Shandong 264003, P.R. China

Received November 7, 2022; Accepted April 11, 2023

DOI: 10.3892/etm.2023.11989

**Abstract.** Vascular remodeling caused by vascular injury such as hypertension and atherosclerosis is a complex process involving a variety of cells and factors, and the mechanism is unclear. A vascular injury model was simulated by adding norepinephrine (NE) to culture medium of vascular adventitial fibroblasts (AFs). NE induced activation and proliferation of AFs. To investigate the association between the AFs activation and bone marrow mesenchymal stem cells (BMSCs) differentiation in vascular remodeling. BMSCs were cultured with supernatant of the AFs culture medium. BMSC differentiation and migration were observed by immunostaining and Transwell assay, respectively, while cell proliferation was measured using the Cell Counting Kit-8. Expression levels of smooth muscle actin ( $\alpha$ -SMA), TGF- $\beta$ 1 and SMAD3 were measured using western blot assay. The results indicated that compared with those in the control group, in which BMSCs were cultured in normal medium, expression levels of  $\alpha$ -SMA, TGF- $\beta$ 1 and SMAD3 in BMSCs cultured in medium supplemented with supernatant of AFs, increased significantly (all  $P < 0.05$ ). Activated AFs induced the differentiation of BMSCs into vascular smooth muscle-like cells and promoted proliferation and migration. AFs activated by NE may induce BMSCs to participate in vascular remodeling. These findings may help

design and develop new approaches and therapeutic strategies for vascular injury to prevent pathological remodeling.

## Introduction

At present, cardiovascular diseases are among the leading causes of death worldwide. A growing body of evidence indicates an association between stem progenitor cells and vascular disease. Several studies indicated that the origin, differentiation and abnormal function of stem/progenitor cells may be key factors in the occurrence and development of cardiovascular disease (1-3). Vascular wall remodeling following vascular injury may contribute to a number of cardiovascular diseases, including atherosclerosis, hypertension and restenosis following vascular reconstruction (4,5). Past studies focused on vascular endothelial cells and vascular smooth muscle cells (VSMCs), but more recently, the role of the adventitia in vascular remodeling has attracted increasing attention (6,7). Adventitial fibroblasts (AFs) are one of the principal cells of the adventitia. Early atherosclerosis is results in proliferation of adventitia rather than the intima and AFs are activated and transformed into myofibroblasts, which express  $\alpha$ -smooth muscle actin (SMA) and migrate to the subintima (8,9). Atherosclerosis is characterized by abundant vasa vasorum in the adventitia; neo-proliferative vasa vasorum develops in the adventitia of the arteries at an early stage (10). Stem/progenitor cells from the adventitia of the arteries and bone marrow-derived stem cells migrate into the intima via the vasa vasorum to participate in vascular remodeling. AFs activated by vascular injury secrete large amounts of matrix and collagen and abnormally express a number of adhesion factors and cytokines, such as increased secretion of TGF- $\beta$ 1 (11,12), some of which may contribute to stem cell mobilization and homing (13,14).

Norepinephrine (NE) is a neurohumoral regulating hormone belonging to the catecholamine family. It is mainly released by sympathetic nerve endings as well as by the adrenal medulla in small amounts to exert a strong vasoconstriction effect that is primarily mediated through receptors. There are mainly sympathetic nerve endings located in the adventitia.

*Correspondence to:* Professor Wendan Yuan or Professor Pengchao Du, Institute of Pathology and Pathophysiology, Basic Medical School, Binzhou Medical University, 346 Guanhai Road, Yantai, Shandong 264003, P.R. China  
E-mail: 981713509@qq.com  
E-mail: 252983491@qq.com

\*Contributed equally

**Key words:** bone marrow mesenchymal stem cell, adventitial fibroblast, proliferation, vascular remodeling, norepinephrine, signal transduction

As a result of increased NE release under sympathetic nervous system activation, oxidative stress, infection injury and changes in blood flow dynamics, smooth muscle cells and AFs occur, resulting in vasoconstriction, increased blood pressure, lumen stenosis and vascular remodeling (15,16).

In the present *in vitro* study, NE was added to cell culture medium to activate AFs to differentiate into myoblasts, simulate the micro-environment of vascular injury, investigate if differentiation and migration of bone marrow mesenchymal stem cells (BMSCs) are associated with AFs activation and examine the mechanism by which BMSCs participate in vascular remodeling. The present results may provide novel insight into the mechanisms of restenosis and atherosclerosis development following vascular injury.

## Materials and methods

**Experimental animals.** The Experimental Animal Center of Binzhou Medical University (Yantai, China) provided 36 3-week-old male Sprague Dawley (SD) rats weighing 80-100 g. The animals were housed in standard cages and maintained under standard conditions at constant room temperature of 20-25°C, 40-70% humidity and 12/12-hlight/dark cycle, with unrestricted access to food and water. For anesthesia, 3% pentobarbital sodium (50 mg/kg body weight) was administered intraperitoneally, and SD rats were sacrificed using CO<sub>2</sub> inhalation, with a fill rate of 60% of the chamber volume/min. Death was confirmed using lack of pulse, breathing, corneal reflex, response to a firm toe pinch and graying of the mucous membranes, which conformed to the Action against Medical Accidents Guidelines for the Euthanasia of Animals: 2020 Edition (17). After SD rats were sacrificed, 75% alcohol was used to disinfect them. Under aseptic conditions, bilateral femurs and the thoracic aorta of rats were removed and isolated. The present study was approved by the Animal Ethics Committee of Binzhou Medical University (approval no. 2020105; 10 December 2020).

**Culture and identification of BMSCs.** Cell-adhesive screening was used to isolate and culture BMSCs. The bone marrow of the femur of 6 SD rats was rinsed with L-DMED culture medium (Hangzhou Sijiqing Biological Engineering Materials Co., Ltd.) using a 5 ml syringe, collected in a sterile centrifuge tube and centrifuged in 1,000 x g for 5 min at 4°C. The supernatant was discarded and L-DMED was added to the centrifuge tube with 15% fetal bovine serum (FBS; cat. no. 11011-8611; Hangzhou Sijiqing Biological Engineering Materials Co., Ltd.) and cells were resuspended. The cell concentration was adjusted to 4x10<sup>5</sup>/ml and transferred into a culture flask. The culture medium was changed after 2 days incubation at 37°C with 5% CO<sub>2</sub>, cells in suspension were discarded and the culture was continued for further 2 days. In the following 6 days, the medium was changed every 3 days. Each day, an inverted phase contrast microscope (magnification, x200; Olympus Corporation) was used to observe the proliferation and morphology of the cells. The rapid proliferation of cells occurred due to adhesion to the petri dish bottom. After reaching 70-80% confluence, cells were sub-cultured. Flow cytometry assay (NovoCyte, Agilent; software version no. FlowJo 10.8.1, BD company) was performed to analyze the

cells after they were sub-cultured for 2-3 generations. Cells were collected, washed in cold PBS, centrifuged in 1,500 x g for 5 min at 4°C and re-suspended in cold PBS. Flow cytometry was used to analyze cells that were labeled with CD105, CD44, and CD34 antibodies (all 1:1,000; cat. nos. A02997-2, A00052 and A00885-1, respectively; all Boster Biological Technology).

**Culture and identification of AFs.** Under aseptic conditions, the adventitia of the thoracic aorta of the rats was isolated from the media and intima. The adventitia was then cut into 0.5-1 mm thick tissue pieces and cultured with complete medium supplemented with 15% FBS. The primary culture of AFs adopted the tissue block adherent culture method, in which pieces were stored in a petri dish and cultivated in an incubator for 2-3 days at 37°C. After being detached from the tissue block, the cells started dividing and proliferating. For 6-7 days, the cells were added to the bottom of the flask, digested and sub-cultured using 0.08% trypsinase (Hangzhou Sijiqing Biological Engineering Materials Co., Ltd.), and the culture medium was changed every other day. AFs at generation 2-3 and 70-80% confluence were sub-cultured in 6-well plates filled with culture medium supplemented with 10% FBS at a density of 1x10<sup>4</sup> cells/cm<sup>2</sup>. After washing three times with PBS, fixing with 4% paraformaldehyde at room temperature for 15 min, immunocytochemical staining was performed to identify the AFs using 1:100 rabbit anti-Vimentin primary antibody (cat. no. PB9359, Boster Biological Technology). The cells in the plate were washed in PBS, and endogenous peroxidase activities were blocked by 3% H<sub>2</sub>O<sub>2</sub> at room temperature for 15 min. After washing with PBS three times, the plates were blocked with goat serum at room temperature for 20 min. Subsequently, the liquid was discarded and the plate dried. The cells were incubated over night at 4°C with the primary antibody followed by incubation with FITC-conjugated goat anti-rabbit secondary antibody (1:3,000; cat. no. A0562, Beyotime Institute of Biotechnology) for 30 min at 37°C. The immunofluorescence was observed using a laser confocal microscope (magnification, x200; FV3000; Olympus Corporation).

**Culture of BMSCs in supernatant of the AFs.** A vascular injury model was simulated *in vitro* and BMSCs at generation 2-3 were co-cultured with the supernatant of the AFs culture medium. L-DMED supplemented with 10% FBS was used as a complete culture medium and maintained at 37°C with 5% CO<sub>2</sub>. These conditions were used for all incubations. In Model 1, AFs were cultured for 2 days in complete culture medium supplemented with NE (cat. no. N7960; Beijing Solarbio Biological Technology) at a final concentration of 10 ng/ml. Subsequently, the medium was replaced with a fresh complete culture medium without NE. Cells were cultured for 1 day and supernatant of the culture medium was collected. BMSCs were cultured with supernatant for 6 days and the AFs supernatant was changed every other day. In Model 2, AFs were cultured for 2 days in complete culture medium without NE, followed by 1 day in fresh complete culture medium and supernatant collection. BMSCs were cultured with the AFs supernatant for 6 days and the supernatant was changed every other day. In the control group, BMSCs were cultured for 6 days in complete culture medium without the supernatant of AFs. The complete

culture medium was changed every other day. An inverted optical light microscope (magnification, x200) was used to observe the morphological changes of BMSCs cultured in AFs supernatant for 6 days. BMSCs from the three groups were collected and washed with PBS to be used in subsequent experiments

**Immunofluorescence of BMSCs.** BMSCs were fixed with 4% paraformaldehyde for 10 min at room temperature. BMSC nuclei were stained with DAPI (0.02 g/l; Santa Cruz Biotechnology, Inc.) overnight at 4°C and incubated with rabbit anti- $\alpha$ -SMA, TGF- $\beta$ 1 and SMAD3 (1:200; cat. nos. AF0048, AF0297 and AF1501, respectively; Beyotime Institute of Biotechnology) primary antibodies at 37°C for 60 min, followed by incubation with FITC- or Cy3-conjugated goat anti-rabbit IgG (1:300; cat. no. A 0562, A0516; Beyotime Institute of Biotechnology) secondary antibodies at 37°C for 60 min. Stained cells were observed under a laser confocal microscope (magnification, x200; FV3000; Olympus Corporation).

**Western blot analysis.** Total protein was extracted from BMSCs using ice-cold RIPA lysis buffer supplemented with 1 mM phenyl methane sulfonyl fluoride (Beyotime Institute of Biotechnology). Total protein was quantified using the Enhanced BCA Protein Assay kit (cat. no. P0006; Beyotime Institute of Biotechnology) and 40  $\mu$ g protein/lane was separated by SDS-PAGE on 8-12% gel. The separated proteins were transferred onto a polyvinylidene fluoride membrane (EMD Millipore; Millipore Sigma) and blocked with 5% skimmed milk for 15 min at room temperature. Membranes were incubated with rabbit anti- $\alpha$ -SMA, anti-TGF- $\beta$ 1, anti-SMAD3 and GAPDH (1:1,000; cat. nos. AF0048, AF0297, AF1501 and AF1186, respectively; Beyotime Institute of Biotechnology) primary antibodies at 4°C overnight. Following primary incubation, membranes were incubated with the horseradish peroxidase-conjugated goat anti-rabbit IgG (1:3,000; cat. no. SA00001-2, Proteintech Group, Inc.) secondary antibody at room temperature for 2 h. The bands were visualized using Millipore Immobilon ECL (Cat. No. WBKLS0100, Millipore Sigma). Protein expression was quantified using Scion Image (version 1.8.0; Scion Corporation) with GAPDH as the loading control.

**Proliferation of BMSCs.** BMSCs in the logarithmic growth phase were seeded into 96-well plates at a density of  $5 \times 10^3$  cells/well (100  $\mu$ l/well). The cells were cultured at 37°C with 5% CO<sub>2</sub> for 12, 24, 36 and 48 h to ensure that they adhered to the plate wall. Cell Counting Kit-8 (CCK-8) reagent (10  $\mu$ l; cat. no. c0037, Beyotime Institute of Biotechnology) was added to each well and incubated for 4 h. A Bio-Tek microplate reader (TecanGroup, Ltd.) was used to measure the absorbance at 450 nm for the determination of BMSC proliferation.

**Migration of BMSCs.** Transwell plates with 8  $\mu$ m pore membranes were used to investigate the BMSC migration. In Model 1, AFs were cultured in complete culture medium with 10 ng/ml NE for 2 days, whereas in Model 2 the AFs were cultured in the complete culture medium without NE for 2 days as afore mentioned. The AFs in Model 1 and 2 were

then centrifuged in 1,500 x g for 5 min at 4°C and rinsed with PBS solution and the AFs were added separately into the lower chamber of the Transwell plate, while the upper chamber was seeded with  $2 \times 10^5$  cells/cm<sup>2</sup>. For the control group, BMSCs ( $2 \times 10^5$  cells/cm<sup>2</sup>) were cultured in the upper chamber without AFs in the lower chamber. BMSCs in the three groups were cultured in the complete culture medium at 37°C with 5% CO<sub>2</sub> for 6 days to observe morphological changes, proliferation and migration under an inverted microscope. The membrane was collected and the cells on the upper surface of the membrane were removed with cotton swabs. The membrane was washed with PBS and cells adhering to the membrane were fixed with 4% paraformaldehyde at room temperature for 15 min. BMSC nuclei were stained with DAPI (0.02 mg/ml; cat. no. c1002; Beyotime Institute of Biotechnology) overnight at 4°C and rinsed five times with PBS to wash away the unbound DAPI. Stained cells were observed in five randomly selected fields of view under laser confocal microscopy (magnification, x100) to measure the migration of BMSCs.

**Statistical analysis.** Data are presented as the mean  $\pm$  standard error of six independent experimental repeats. The significance of the differences was examined by one-way ANOVA followed by Duncan's multiple range tests. Statistical analysis was performed using SPSS20.0 (IBM Corp.) and GraphPad Prism 6 (GraphPad Software; Dotmatics000.0). P<0.05 was considered to indicate a statistically significant difference.

## Results

**Morphology and immunofluorescence of BMSCs.** By using the cell adherent screening method, BMSCs were isolated, cultured and observed under an inverted microscope. After 3 days of culture, round monocytes adhered to the wall, whereas hematopoietic stem cells did not adhere to the wall, allowing them to be discarded in the exchange fluid of culture medium. The primary culture of BMSCs showed a short shape and mostly round and unextended. A few extended cells started to appear and proliferate at 3-5 days. Cells were typically spindle-shaped with 2-3 long protrusions, while a few cells were polygonal and rod-shaped with large oblate nuclei and 1-2 nucleoli (Fig. 1A). Cells were sub-cultured after 5-6 days of cell culture. In cell culture, cell morphology gradually homogenized into long spindle shape, cells proliferated rapidly and exhibited swirls (Fig. 1B). As soon as 2-3 generations of BMSCs were obtained, flow cytometry analysis revealed that the BMSCs were negative for CD34, while they were positive for CD44 and CD105 (Fig. 1C). According to these findings, cultured cells had morphological and immunophenotypical characteristics similar to those of BMSCs.

**Morphology and immunofluorescence of AFs.** As observed under an inverted microscope, AFs grew from the edge of the vascular adventitial tissue block and divided 2-3 days later. The primary cultured AFs also demonstrated adherent growth with large and oblate nuclei (Fig. 2A). Under the microscope, the adherent cells were irregular polygons or fusiform, growing vigorously and overlapping in crista-like layers (Fig. 2B). Fluorescence staining indicated that AFs cells were positive for vimentin expression (Fig. 2C).

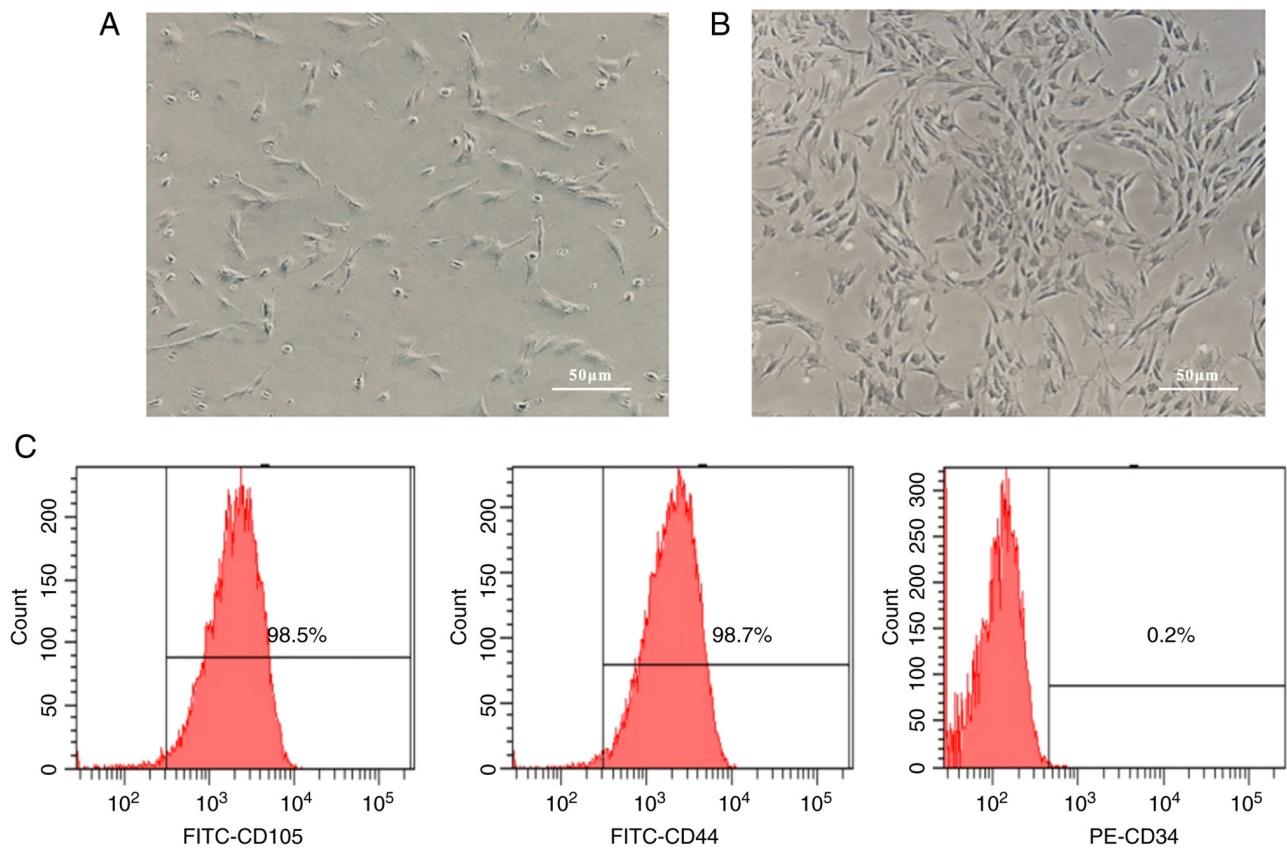


Figure 1. Identification of cultured BMSCs and morphological characteristics. (A) Adhesion was observed on the petri dish of BMSCs in primary culture. (B) BMSCs transformed into long, vortex-shaped spindles after 2-3 generations. (C) Flow cytometry results of the identification of BMSCs. The corresponding positive cells accounted for 98.5, 98.7 and 0.2%. BMSC, bone marrow stem cell.

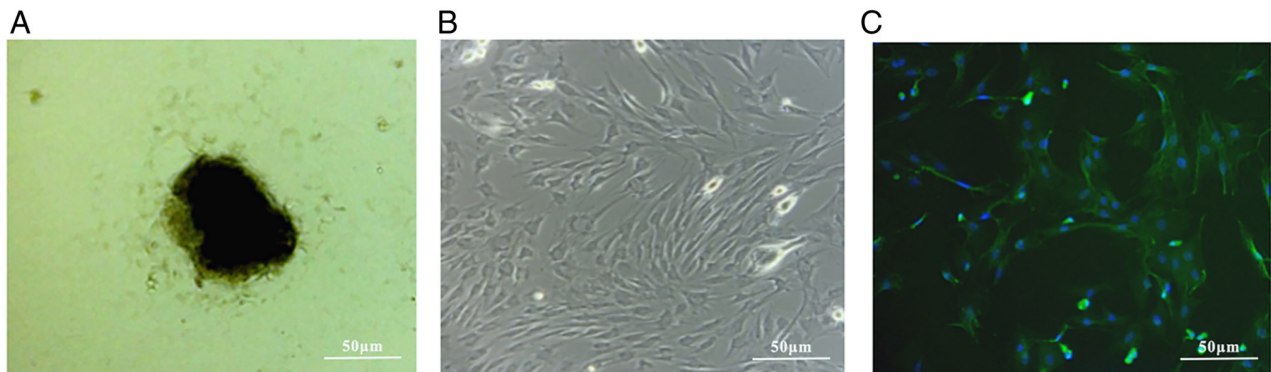


Figure 2. Culture and identification of vascular adventitial fibroblasts. (A) Up on culturing vascular tissue fragments for 2-3 days, fibroblasts grew from the edges of each fragment and primary cultured AFs were adherent in irregular polygonal shapes. (B) At generations 2-3, fibroblasts proliferated rapidly, exhibiting strong growth and multilayer over lapping crest patterns. (C) Vimentin-positive AFs showed green fluorescence. AF, adventitial fibroblast.

**Morphology and immunofluorescence identification of BMSCs cultured in AFs supernatant.** Induction and differentiation of BMSCs were performed using cells at generations 2-3. An inverted microscope was used to observe the morphology of the cultured cells. After 6 days of BMSCs culture with supernatant of AFs, the BMSCs had exhibited 70-80% confluence in Models 1 and 2. BMSCs morphology had lost the characteristic swirls state, while some cells changed their long spindle shape and exhibited an elliptical appearance. There was no notable change in cell morphology in the control group. A total of three groups of cell slides were prepared

for immunofluorescence staining. The cytoplasm expressing  $\alpha$ -SMA showed red fluorescence due to the Cy3-conjugated second antibody goat anti-rabbit IgG, while positive expression of TGF- $\beta$ 1 and SMAD3 in the cytoplasm was indicated by a green fluorescence due to the FITC-conjugated secondary goat anti-rabbit IgG. Immunofluorescence showed that after cell culture for 6 days, Model 1 exhibited the strongest staining compared with that in model 2 and the Control group (Fig. 3A).

**Western blot analysis.** Western blotting was used to analyze expression of  $\alpha$ -SMA and TGF- $\beta$ 1/SMAD3 signaling pathway



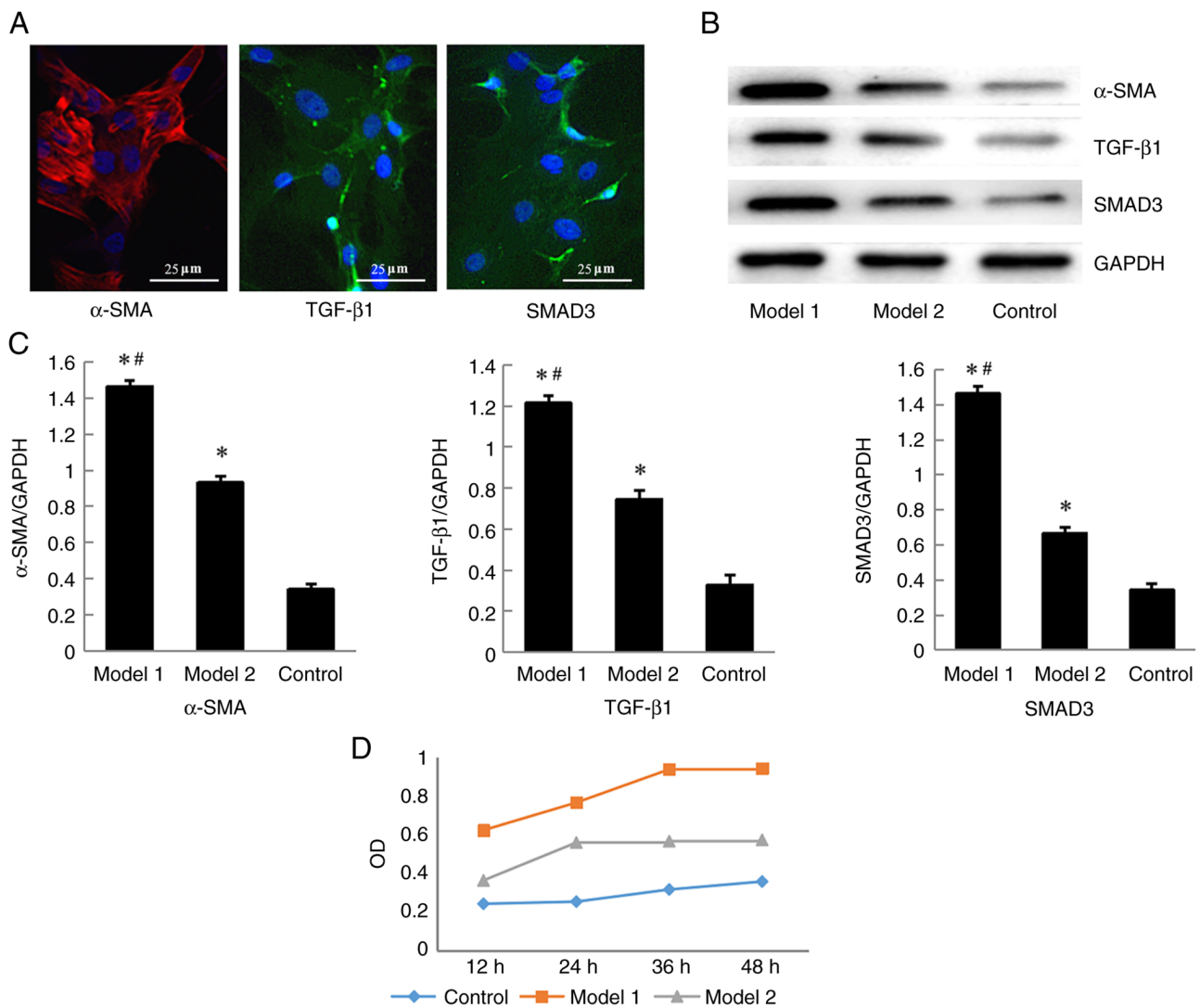


Figure 3. Identification of BMSCs by immunofluorescence and western blotting. (A) Immunofluorescence staining of BMSCs in Model 1 (red,  $\alpha$ -SMA; green, TGF- $\beta$ 1 and SMAD3; blue, nuclei). (B) Protein expression of  $\alpha$ -SMA, TGF- $\beta$ 1 and SMAD3 in BMSCs shown by the western blot analysis. (C) Quantification of the western blot assay. Data are presented as the mean  $\pm$  standard deviation (n=6). \*P<0.05 vs. control. #P<0.05 model 1 vs. model 2. (D) Proliferation of BMSCs was significantly different among the three groups as assessed using the Cell Counting Kit-8 assay. BMSC, bone marrow stem cell;  $\alpha$ -SMA, smooth muscle actin; OD, optical density.

proteins in the BMSCs (Fig. 3B). Models 1 and 2 differed significantly from the control (P<0.05). Compared with those in the control group, the expression levels of  $\alpha$ -SMA, TGF- $\beta$ 1 and SMAD3 in BMSCs in models 1 and 2 were increased (P<0.05; Fig. 3C), with model 1 showing the highest increase.

**Proliferation of BMSCs.** The proliferation of BMSCs was evaluated using the CCK-8 method. BMSCs from Model 1 and 2 were cultured with AFs supernatant for 12, 24, 36 and 48 h, while BMSCs cultured in normal medium were used as the control group (Fig. 3D). There were all have significant differences among the three groups of the proliferation of BMSCs (P<0.05), and the Model 1 showing the highest proliferation rate.

**Migration of BMSCs.** According to Transwell migration assay, BMSCs migrated from the upper to the lower chamber through the membrane in all three groups. BMSCs migration in Model 1 was significantly higher than that in Model 2 and Control after 6 days of culture (P<0.05; Fig. 4A and B).

## Discussion

At present, the incidence of cardiovascular diseases is increasing globally, which accounts for a large proportion of the global disease burden, nearly doubling from 271 million in 1990 to 523 million in 2019, and the mortality rate is also on the rise (18). Atherosclerosis is the most common cause of cardiovascular disease, including intima injury, vascular wall pathological remodeling and lumen stenosis (19,20). It is hypothesized that cell proliferation in the intima and media of arteries contributes to vascular remodeling, whereas the adventitia of the arteries is not involved (21). It is hypothesized that the adventitia provides only physical and nutritional support to the vascular wall. In addition to being composed of loose connective tissue, the adventitia is rich in vasa vasorum, lymphatic vessels and adrenergic nerves and is surrounded by perivascular adipose tissue (8). A previous study demonstrated that various cells in the adventitia of the blood vessels, particularly fibroblasts, have high metabolic activity (22). Secretion

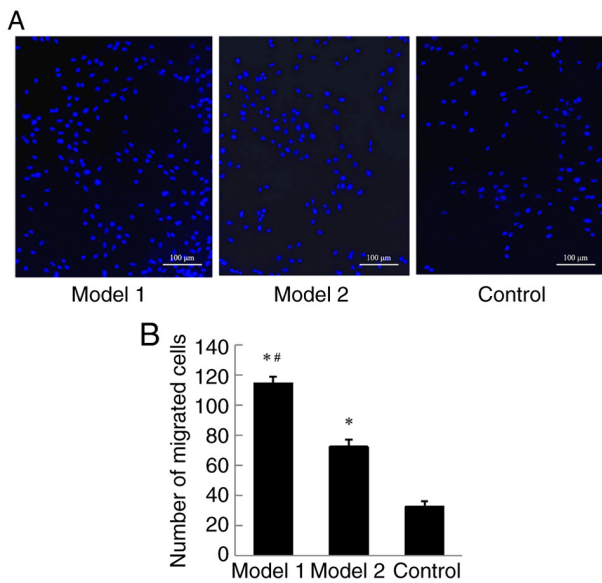


Figure 4. Migration and proliferation of BMSCs. (A) Fluorescence of DAPI-labeled migrated BMSCs nuclei is shown in blue. Model 1 showed the highest migration rate. (B) Number of BMSCs that migrated after 6 days of culture. Data are presented as the mean  $\pm$  standard deviation (n=6). \*P<0.05 vs. control. #P<0.05 Model 1 vs. Model 2. BMSC, bone marrow stem cell.

of numerous cytokines, enzymes and chemokines by AFs following injury is increased compared with smooth muscle cells. These cytokines, enzymes and chemokines, including TGF- $\beta$ 1, monocyte chemotactic protein-1, interleukins, TNF- $\alpha$ , endothelin-1 and matrix metallo proteinases, induce an inflammatory response and vascular remodeling (23), which may contribute to the mobilization of stem cells. Previous studies have demonstrated that the source of vascular remodeling of smooth muscle cells following vascular injury is not only the cells of the vascular wall itself but some BMSCs are also involved through adhesion differentiation (24,25). Ni *et al* (26) reported that TGF- $\beta$ 1 expression was increased in neointimal lesion of transplanted angiogenesis, and TGF- $\beta$ 1 stimulated c-kit + cells to differentiate into smooth muscle cells. It is hypothesized that proliferating smooth muscle cells in damaged blood vessels are derived from stem/progenitor cells that exist *in situ* within the vessel wall (3). A previous study demonstrated MMP8 secreted by macrophages promotes the differentiation of vasculo membrane stem cells into smooth muscle cells by TGF- $\beta$  and expression of  $\alpha$ -SMA gene by binding the binding site of the smooth muscle cell gene promoter through NOTCH1; moreover, vascular injury disease is associated with neointimal hyperplasia caused by differentiation of adventitial membrane stem cells into smooth muscle cells (27). Another study showed that Dickkopf-3 induced the differentiation of Spinocerebellar ataxia type 1-positive vascular progenitor cells into smooth muscle cells via the activation of TGF- $\beta$ /activating transcription factor 6 and Wnt signaling pathways, leading to maintenance of atherosclerotic plaque stability (28).

BMSCs are among the most studied mesenchymal stem cells due to their relatively simple culture, fast proliferation, high genetic stability, ability to multi-differentiate and low immunogenicity (29). The primary pathological target cells for vascular remodeling are VSMCs, although, some studies have

suggested that vascular stem/progenitor cells may contribute to smooth muscle cell development in vascular remodeling lesions (30). Due to their complexity, the origins of these stem/progenitor cells and their inducer remains unclear; therefore; discovering the key inducer of stem/progenitor cells is important. According to a previous study, miR-503 promoted the mesenchymal stem cell differentiation induced by TGF- $\beta$ 1 in a VSMC model by targeting SMAD7 (31). In addition, miR-128 inhibited the differentiation of human hair follicle mesenchymal dry cells into smooth muscle induced by TGF- $\beta$ 1 by targeting SMAD2 (32).

Our previous study examined the interaction between BMSCs and AFs to discover the mechanism of cell differentiation and vascular remodeling (33). In response to vascular injury, certain cytokines and chemokines mobilize stem/progenitor cells into the local adhesion of the injury (34). Among these, TGF- $\beta$ 1 was shown to play a fundamental role as it promoted cell proliferation, migration and stroma secretion and was involved in vascular remodeling (35,36). In the present study, NE was added to medium to activate AFs, express  $\alpha$ -SMA, differentiate into myoblasts and secrete increased TGF- $\beta$ 1 to simulate *in vitro* the micro-environment of vascular injury. BMSCs were cultured with supernatant of AFs to observe the effect on cell differentiation and migration. After 2 days of culture, BMSCs showed increased expression of  $\alpha$ -SMA, TGF- $\beta$ 1 and SMAD3. According to these findings, NE-induced activation of AFs during vascular injury induced differentiation and migration of BMSCs and facilitated differentiation into smooth muscle-like cells, likely through the TGF- $\beta$ 1/Smad3 signaling pathway involved in vascular remodeling.

An example of a classic neurotransmitter is NE. Sympathetic and parasympathetic nerves are primarily distributed in the vascular adventitia. Catecholamines, such as NE, are released from sympathetic nerve extremities and diffuse or enter the bloodstream to act on VSMCs and endothelial cells. As an  $\alpha$ - and  $\beta$ -receptor agonist, NE plays an important role in the regulation of the cardiovascular system (37). Sympathetic activity is directly associated with the plasma NE levels and the severity of hypertension (38). The implementation of device-based therapeutic interventions to decrease renal and systemic sympathetic activity is used to attenuate hypertension in patients with resistant hypertension. This technique aims to decrease renal sympathetic activation by the destruction of renal sympathetic nerves located in the adventitia of the renal artery (39). A previous study demonstrated that NE induces epithelial-mesenchymal transformation of lung cancer cells and promotes invasion and metastasis of lung cancer via the TGF- $\beta$ 1 signaling pathway (40). CD147 expression upregulated by stress hormone NE via the  $\beta$ -adrenergic/ $\beta$ -arrestin1/ERK1/2-selective promoter factor 1 pathway promotes secretion of MMP-2 and levels of extracellular lactic acid, which accelerates invasion and metastasis of glioma cells *in vitro* (41). NE is released from the sympathetic ends of the heart and exerts its biological role by stimulating cardiac adrenergic receptors (42). A recent study showed that NE-induced activation of AFs of rats promoted AFs phenotypical transformation and proliferation, which was mediated by  $\alpha$ -receptor (16,43). NE promotes AFs-derived small extracellular vesicle release of angiotensin converting

enzyme. miR-155-5p and miR-135a-5p, which were detected in extracellular vesicles using reverse transcription-quantitative PCR, were shown to be involved in adjusting VSMC proliferation in hypertension (16).

Sympathetic nerve endings, which are primarily located in the arterial vascular adventitia, release NE. The sympathetic nerves primarily innervate the adventitia of the artery but rarely innervate the media of the artery (44). However, as a key regulator in neurohumoral regulation, the roles of NE in vascular adventitia remain unclear. To the best of our knowledge, the present study is the first to use NE to promote the activation of AFs, which induced differentiation and migration of BMSCs via the vascular remodeling process. This finding suggested that inhibition of NE-induced activation may be a potential therapeutic target for excessive sympathetic activation-associated vascular remodeling.

According to a previous study (45), early implementation of certain interventions in the adventitia may delay or suspend the process of atherosclerotic vascular remodeling. Adventitial Sca1+ cells transduced with ETV2 are committed to the endothelial fate and improve vascular remodeling following injury. However, stem cell migration and differentiation are influenced by several factors and are complex processes, such as smooth muscle derived chemokines CCL2 and CXCL1 induced vascular stem/progenitor cell contributes to neointima formation (23). It has been reported that DKK3 (Dkkopf-3) transdifferentiates fibroblasts into functional endothelial cells (46). DKK3 alters atherosclerotic plaque phenotype involving vascular progenitor and fibroblast differentiation into smooth muscle (28). So on the one hand, activated stem cells contribute to the repair of damaged tissue; on the other hand, these cells may contribute to vascular remodeling and aggravate atherosclerosis. Therefore, it is essential to have a thorough understanding of the mechanism of stem cell migration and differentiation in pathological conditions to improve the understanding of the pathogenesis of cardiovascular disease, discover new targets and provide novel preventive strategies

## Acknowledgements

Not applicable.

## Funding

The present study was supported by the Natural Science Foundation of Shandong Province (grant nos. ZR2017MH046 and ZR2020MH080) and the Science Foundation of Binzhou Medical University (grant nos. BY2020KJ46, BY2019XRX06 and BY2019XRX07).

## Availability of data and materials

The dataset used and/or analyzed during the current study are available from the corresponding author on reasonable request.

## Authors' contributions

WY, DY and JG were responsible for study design, data collection, statistical analysis and manuscript preparation. LL, DZ and LC were responsible for data collection,

statistical analysis and literature search. XS, XW, PD and WY supervised the project, designed the study, analyzed data and wrote the manuscript. All authors have read and approved the final manuscript. WY and PD confirm the authenticity of all raw data.

## Ethics approval and consent to participate

The present study was approved by the Institutional Animal Care and Use Committee of Binzhou Medical University (approval no. 2015-008).

## Patient consent for publication

Not applicable.

## Competing interests

The authors declare that they have no competing interests.

## References

1. Yu B, Chen Q, Le Bras A, Zhang L and Xu Q: Vascular stem/progenitor cell migration and differentiation in atherosclerosis. *Antioxid Redox Signal* 29: 219-235, 2018.
2. Jiang L, Sun X, Deng J, Hu Y and Xu Q: Different roles of stem/progenitor cells in vascular remodeling. *Antioxid Redox Signal* 35: 192-203, 2021.
3. Zhang L, Issa Bhaloo S, Chen T, Zhou B and Xu Q: Role of resident stem cells in vessel formation and arteriosclerosis. *Circ Res* 122: 1608-1624, 2018.
4. Wang D, Wang Z, Zhang L and Wang Y: Roles of cells from the arterial vessel wall in atherosclerosis. *Mediators Inflamm* 2017: 8135934, 2017.
5. Durham AL, Speer MY, Scatena M, Giachelli CM and Shanahan CM: Role of smooth muscle cells in vascular calcification: Implications in atherosclerosis and arterial stiffness. *Cardiovasc Res* 114: 590-600, 2018.
6. Patzelt M, Kachlik D, Stingl J, Sach J, Stibor R, Benada O, Kofronova O and Musil V: Morphology of the vasa vasorum in coronary arteries of the porcine heart: A new insight. *Ann Anat* 223: 119-126, 2019.
7. Chen Y, Chen Y, Jiang X, Shi M, Yang Z, Chen Z, Hua X, Chen J and Wang Y: Vascular adventitial fibroblasts-derived FGF10 promotes vascular smooth muscle cells proliferation and migration in vitro and the neointima formation in vivo. *J Inflamm Res* 25: 2207-2223, 2021.
8. Nava E and Llorens S: The local regulation of vascular function: From an inside-outside to an outside-inside model. *Front Physiol* 10: 729, 2019.
9. Zou F, Li Y, Zhang S and Zhang J: DP1 (prostaglandin D2 receptor 1) activation protects against vascular remodeling and vascular smooth muscle cell transition to myofibroblasts in angiotensin II-induced hypertension in mice. *Hypertension* 79: 1203-1215, 2022.
10. Sedding DG, Boyle EC, Demandt JAF, Sluimer JC, Dutzmann J, Haverich A and Bauersachs J: Vasa vasorum angiogenesis: Key player in the initiation and progression of atherosclerosis and potential target for the treatment of cardiovascular disease. *Front Immunol* 9: 706, 2018.
11. Li XD, Hong MN, Chen J, Lu YY, Ye MQ, Ma Y, Zhu DL and Gao PJ: Adventitial fibroblast-derived vascular endothelial growth factor promotes vasa vasorum-associated neointima formation and macrophage recruitment. *Cardiovasc Res* 116: 708-720, 2020.
12. Hu HH, Chen DQ, Wang YN, Feng YL, Cao G, Vaziri ND and Zhao YY: New insights into TGF- $\beta$ /Smad signaling in tissue fibrosis. *Chem Biol Interact* 292: 76-83, 2018.
13. Yang JX, Pan YY, Wang XX, Qiu YG and Mao W: Endothelial progenitor cells in age-related vascular remodeling. *Cell Transplant* 27: 786-795, 2018.



14. Lv BK, Li F, Fang J, Xu L, Sun C, Han J, Hua T, Zhang Z, Feng Z and Jiang X: Hypoxia inducible factor 1 $\alpha$  promotes survival of mesenchymal stem cells under hypoxia. *Am J Transl Res* 9: 1521-1529, 2017.
15. DeLalio LJ, Sved AF and Stocker SD: Sympathetic Nervous system contributions to hypertension: Updates and therapeutic relevance. *Can J Cardiol* 36: 712-720, 2020.
16. Ye C, Zheng F, Xu T, Wu N, Tong Y, Xiong XQ, Zhou YB, Wang JJ, Chen Q, Li YH, *et al*: Norepinephrine acting on adventitial fibroblasts stimulates vascular smooth muscle cell proliferation via promoting small extracellular vesicle release. *Theranostics* 12: 4718-4733, 2022.
17. Leary S, Underwood W, Anthony R, *et al*: AVMA Guidelines for the euthanasia of animals: 2020 Edition. Schaumburg: American Veterinary Medical Association, 2020.
18. Roth GA, Mensah GA, Johnson CO, Addolorato G, Ammirati E, Baddour LM, Barengo NC, Beaton AZ, Benjamin EJ, Benziger CP, *et al*: Global Burden of cardiovascular diseases and risk factors, 1990-2019: Update From the GBD 2019 study. *J Am Coll Cardiol* 76: 2982-3021, 2020.
19. Soehnlein O and Libby P: Targeting inflammation in atherosclerosis from experimental insights to the clinic. *Nat Rev Drug Discov* 20: 589-610, 2021. Lee J and Choi JH: Deciphering macrophage phenotypes upon lipid uptake and atherosclerosis. *Immune Netw* 20: e22, 2020.
20. Ma Z, Mao C, Jia Y, Fu Y and Kong W: Extracellular matrix dynamics in vascular remodeling. *Am J Physiol Cell Physiol* 319: C481-C499, 2020.
21. Tinajero MG and Gotlieb AI: Recent developments in vascular adventitial pathobiology: The dynamic adventitia as a complex regulator of vascular disease. *Am J Pathol* 190: 520-534, 2020.
22. Han X, Wu A, Wang J, Chang H, Zhao Y, Zhang Y, Mao Y, Lou L, Gao Y, Zhang D, *et al*: Activation and migration of adventitial fibroblasts contributes to vascular remodeling. *Anat Rec (Hoboken)* 301: 1216-1223, 2018.
23. Yu B, Wong MM, Potter CM, Simpson RM, Karamariti E, Zhang Z, Zeng L, Warren D, Hu Y, Wang W and Xu Q: Vascular stem/progenitor cell migration induced by smooth muscle cell-derived chemokine (C-C Motif) ligand 2 and chemokine (C-X-C motif) ligand 1 contributes to neointima formation. *Stem Cells* 34: 2368-2380, 2016.
24. Gu W, Nowak WN, Xie Y, Le Bras A, Hu Y, Deng J, Issa Bhaloo S, Lu Y, Yuan H, Fidanis E, *et al*: Single-Cell RNA-Sequencing and metabolomics analyses reveal the contribution of perivascular adipose tissue stem cells to vascular remodeling. *Arterioscler Thromb Vasc Biol* 39: 2049-2066, 2019.
25. Iso Y, Usui S, Toyoda M, Spees JL, Umezawa A and Suzuki H: Bone marrow-derived mesenchymal stem cells inhibit vascular smooth muscle cell proliferation and neointimal hyperplasia after arterial injury in rats. *Biochem Biophys Res* 16: 79-87, 2018.
26. Ni Z, Deng J, Potter CMF, Nowak WN, Gu W, Zhang Z, Chen T, Chen Q, Hu Y, Zhou B, *et al*: Recipient c-Kit lineage cells repopulate smooth muscle cells of transplant arteriosclerosis in mouse models. *Circ Res* 125: 223-241, 2019.
27. Yang F, Chen Q, Yang M, Maguire EM, Yu X, He S, Xiao R, Wang CS, An W, Wu W, *et al*: Macrophage-derived MMP-8 determines smooth muscle cell differentiation from adventitia stem/progenitor cells and promotes neointima hyperplasia. *Cardiovasc Res* 116: 211-225, 2020.
28. Karamariti E, Zhai C, Yu B, Qiao L, Wang Z, Potter CMF, Wong MM, Simpson RML, Zhang Z, Wang X, *et al*: DKK3 (Dickkopf 3) Alters atherosclerotic plaque phenotype involving vascular progenitor and fibroblast differentiation into smooth muscle cells. *Arterioscler Thromb Vasc Biol* 38: 425-437, 2018.
29. Gong P, Zhang W, He Y, Wang J, Li S, Chen S, Ye Q and Li M: Classification and characteristics of mesenchymal stem cells and its potential therapeutic mechanisms and applications against ischemic stroke. *Stem Cells Int* 2021: 2602871, 2021.
30. Wang H, Zhao H, Zhu H, Li Y, Tang J, Li Y and Zhou B: Sc $\alpha$ 1 + cells minimally contribute to smooth muscle cells in atherosclerosis. *Circ Res* 128: 133-135, 2021.
31. Gu X, Hong X, Bras AL, Le Bras A, Nowak WN, Issa Bhaloo S, Deng J, Xie Y, Hu Y, Ruan XZ and Xu Q: Smooth muscle cells differentiated from mesenchymal stem cells are regulated by microRNAs and suitable for vascular tissue grafts. *J Biol Chem* 293: 8089-8102, 2018.
32. Wang Z, Pang L, Zhao H, Song L, Wang Y, Sun Q, Guo C, Wang B, Qin X and Pan A: miR-128 regulates differentiation of hair follicle mesenchymal stem cells into smooth muscle cells by targeting SMAD2. *Acta Histochem* 118: 393-400, 2016.
33. Wendan Y, Changzhu J, Xuhong S, Hongjing C, Hong S, Dongxia Y and Fang X: BMSCs interactions with adventitial fibroblasts display smooth muscle cell lineage potential in differentiation and migration that contributes to neointimal formation. *Stem Cells Int* 2016: 3196071, 2016.
34. Lu W and Li X: Vascular stem/progenitor cells: Functions and signaling pathways. *Cell Mol Life Sci* 75: 859-869, 2018.
35. Low EL, Baker AH and Bradshaw AC: TGF $\beta$ , smooth muscle cells and coronary artery disease: A review. *Cell Signal* 53: 90-101, 2019.
36. Kudryashova TV, Shen Y, Pena A, Cronin E, Okorie E, Goncharov DA and Goncharova EA: Inhibitory antibodies against activin A and TGF $\beta$  reduce self-supported, but not soluble factors-induced growth of human pulmonary arterial vascular smooth muscle cells in pulmonary arterial hypertension. *Int J Mol Sci* 19: 2957, 2018.
37. Grassi G, Pisano A, Bolignano D, Seravalle G, D'Arrigo G, Quarti-Trevano F, Mallamaci F, Zoccali C and Mancina G: Sympathetic nerve traffic activation in essential hypertension and its correlates: Systematic reviews and meta-analyses. *Hypertension* 72: 483-491, 2018.
38. Oparil S, Acelajado MC, Bakris GL, Berlowitz DR, Cifková R, Dominiczak AF, Grassi G, Jordan J, Poulter NR, Rodgers A and Whelton PK: Hypertension. *Nat Rev Dis Primers* 4: 18014, 2018.
39. Akinseye OA, Ralston WF, Johnson KC, Ketron LL, Womack CR and Ibebuogu UN: Renal sympathetic denervation: A comprehensive review. *Curr Probl Cardiol* 46: 100598, 2021.
40. Zhang J, Deng YT, Liu J, Wang YQ, Yi TW, Huang BY, He SS, Zheng B and Jiang Y: Norepinephrine induced epithelial-mesenchymal transition in HT-29 and A549 cells in vitro. *J Cancer Res Clin Oncol* 142: 423-435, 2016.
41. Wang P, Wang Z, Yan Y, Xiao L, Tian W, Qu M, Meng A, Sun F, Li G and Dong J: Psychological stress up-regulates CD147 expression through Beta-Arrestin1/ERK to promote proliferation and invasiveness of glioma cells. *Front Oncol* 10: 571181, 2020.
42. Lymperopoulos A, Cora N, Maning J, Brill AR and Sizova A: Signalling and function of cardiac autonomic nervous system receptors: Insights from the GPCR signalling universe. *FEBS J* 288: 2645-2659, 2021.
43. Ren XS, Tong Y, Qiu Y, Ye C, Wu N, Xiong XQ, Wang JJ, Han Y, Zhou YB, Zhang F, *et al*: MiR155-5p in adventitial fibroblasts-derived extracellular vesicles inhibits vascular smooth muscle cell proliferation via suppressing angiotensin-converting enzyme expression. *J Extracell Vesicles* 9: 1698795, 2019.
44. Mackay CDA, Jadli AS, Fedak PWM and Patel VB: Adventitial fibroblasts in aortic aneurysm: Unraveling pathogenic contributions to vascular disease. *Diagnostics (Basel)* 12: 871, 2022.
45. Le Bras A, Yu B, Issa Bhaloo S, Hong X, Zhang Z, Hu Y and Xu Q: Adventitial Sc $\alpha$ 1 + cells transduced with ETV2 are committed to the endothelial fate and improve vascular remodeling after injury. *Arterioscler Thromb Vasc Biol* 38: 232-244, 2018.
46. Chen T, Karamariti E, Hong X, Deng J, Wu Y, Gu W, Simpson R, Wong MM, Yu B, Hu Y, *et al*: DKK3 (Dickkopf-3) transdifferentiates fibroblasts into functional endothelial cells-brief report. *Arterioscler Thromb Vasc Biol* 39: 765-773, 2019.



This work is licensed under a Creative Commons Attribution-NonCommercial-NoDerivatives 4.0 International (CC BY-NC-ND 4.0) License.